

# An evolutionary hybrid optimization of MARS model in predicting settlement of shallow foundations on sandy soils

Nguyen-Vu Luat<sup>1a</sup>, Van-Quang Nguyen<sup>2b</sup>, Seunghye Lee<sup>1c</sup>, Sungwoo Woo<sup>3b</sup> and Kihak Lee<sup>\*1</sup>

<sup>1</sup>Department of Architectural Engineering, Sejong University, 209 Neungdong-ro, Gwangjin-gu, Seoul 05006, South Korea

<sup>2</sup>Department of Civil and Environmental Engineering, Hanyang University, 222 Wangsimni-ro, Seongdong-gu, Seoul 04763, South Korea

<sup>3</sup>TechSquare Ltd. South Korea, 25 Banpodae-ro, Seocho-gu, Seoul 06710, South Korea

(Received January 13, 2020, Revised April 21, 2020, Accepted May 18, 2020)

**Abstract.** This study is attempted to propose a new hybrid artificial intelligence model called integrative genetic algorithm with multivariate adaptive regression splines (GA-MARS) for settlement prediction of shallow foundations on sandy soils. In this hybrid model, the evolution algorithm – Genetic Algorithm (GA) was used to search and optimize the hyperparameters of multivariate adaptive regression splines (MARS). For this purpose, a total of 180 experimental data were collected and analyzed from available researches with five-input variables including the breadth of foundation ( $B$ ), length to width ( $L/B$ ), embedment ratio ( $D_f/B$ ), foundation net applied pressure ( $q_{net}$ ), and average SPT blow count ( $N_{SPT}$ ). In further analysis, a new explicit formulation was derived from MARS and its accuracy was compared with four available formulae. The attained results indicated that the proposed GA-MARS model exhibited a more robust and better performance than the available methods.

**Keywords:** multivariate adaptive regression spline; genetic algorithm; evolutionary hybrid model; settlement prediction; shallow foundation

## 1. Introduction

The estimation of foundation settlement is a fundamental and critical subject matter of foundation engineering and is a standard procedure carried out by geotechnical engineers. The settlement of shallow foundations can be classified into three categories: immediate settlement, primary consolidation, and secondary consolidation settlement. The primary consolidation settlement is the result of a volume change in saturated cohesive soils because of the expulsion of the water that occupies the void spaces. In contrast, the secondary consolidation settlement is caused by the plastic adjustment of soil particles. Once the load applies, the immediate settlement is induced by the elastic deformation of dry soil, moist and saturated soils without any change in moisture content. Therefore, it can be computed using elastic theory and applied for all fine-grained soils, including sandy soil. In the past, some simple equations were proposed by Harr (1966) for estimating the immediate settlement for a flexible and rigid foundation, which depicted in Fig. 1. However, due to the heterogeneous nature of the soil, the process of predicting settlement is tedious and complicated. In general, sandy soil has a higher differential settlement

compared to cohesive soils since the former is less homogeneous than the latter. Moreover, the deformation behavior of shallow foundations obtaining their support from granular soils (i.e., sands, gravels) mainly governs the final design of structures that are built on these soil types. Therefore, predicting settlement is a crucial issue and is one of the most significant concerns in foundation design codes.

In the last five decades, numerous studies have been published to examine the correlation between expected settlements and the measured settlement of shallow foundations on cohesionless soils. Some suggested new methods for settlement estimation (Terzaghi and Peck 1968, Schmertmann 1970, Shahin and Jaksa 2006), while others sought to compare various methods to assess whether or not any particular approach offered higher-level accuracy than others (Elton 1987, Mageri *et al.* 1998, Abate *et al.* 2008). The reliability of settlement estimation for shallow foundations on sandy soils also received substantial attention in recent years (Tan and Duncan 1991, Shahin *et al.* 2005). Das and Shivakugan (2007) provided an overview and reported that Shivakugan and Johnson's (2004) probabilistic design chart approach can be used to estimate the likelihood of the actual settlement in the field may exceed 25 mm.

Because of the difficulty of collecting undisturbed samples, the majority of the available methods for the settlement prediction of shallow foundations on sandy soils are based on in-situ tests, such as the pressuremeter test, plate load test, dilatometer test, drive cone test, cone penetration test (CPT) and standard penetration test (SPT) (Meyerhof 1956, 1964, 1974). The obtained results were either utilized: to determine an elastic moduli of soil for elastic deformation analysis; to directly predict settlement

\*Corresponding author, Professor

E-mail: [kihaklee@sejong.ac.kr](mailto:kihaklee@sejong.ac.kr)

<sup>a</sup>Ph.D. Candidate

E-mail: [luatnv@sju.ac.kr](mailto:luatnv@sju.ac.kr)

<sup>b</sup>Ph.D.

<sup>c</sup>Professor

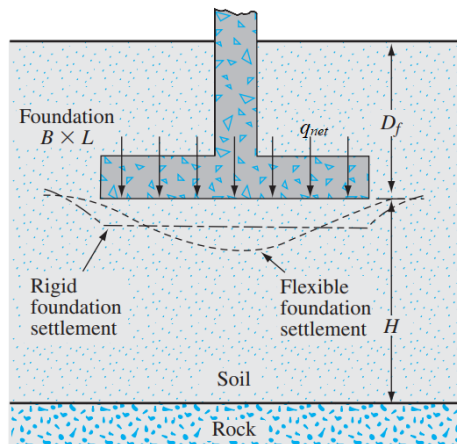


Fig. 1 A rectangular shallow foundation and its immediate settlement on sandy soil (Das *et al.* 2002).  $B$ ,  $L$  – width and length of foundation, respectively;  $q_{net}$  – net applied pressure;  $D_f$  – embedment depth;  $H$  – the distance of footing base to rock surface

based on an empirical relationship; or to estimate other soil properties (i.e., over consolidation ratio, relative density) for settlement estimation. However, most of these approaches attempted to simplify the problem by assuming a linear response between load and deformation and related it to the factors that could affect the settlement value. Therefore, the previous methods failed to find a successful solution for accurately predicting the settlement. In these analysis studies, no specific method was superior to the others in all cases, and the calculated results of the settlement were inconsistent (Alpan 1964, Arnold 1980, Jeyepalan and Boehm 1986, Shahin and Jaksa 2006). Consequently, there remains a need for a more efficient method which can provide settlement prediction results with higher accuracy. To meet this goal, a new approach using the advantage of artificial intelligence (AI) technique was used in this study.

In the last two decades, there have been several applications of AI techniques in predicting settlement of shallow foundation on cohesionless soil, e.g., artificial neural network (ANN) (Shahin *et al.* 2002), support vector machines (SVM) (Samui and Sitharam 2008), *etc.* However, their application has some limitations, such as predicting with moderate accuracy, not showing the relative importance of the input variables, and/or not providing an explicit predictable formula. This paper thus utilizes the Multivariate Adaptive Regression Splines (MARS) model to improve the accuracy of predicting settlement of shallow foundation on sandy soil as well as to propose a new practical equation.

MARS, which was first proposed by Friedman (1991), is capable of fitting non-linear, complex relationships between a set of predictors and dependent variables. The predictors' space is divided into multiple knots in order to fit a spline function between these knots. Some of the main advantages of MARS are the ability to capture the complicated data mapping in high-dimensional patterns and to produce more straightforward, more accurate and faster simulations, and easier-to-elucidate models for both

classification and regression problems. Some previous applications of MARS in geotechnical and structural engineering can be found in several available literatures (Samui 2011, Zhang and Goh 2014, Xiang *et al.* 2018, Zhang *et al.* 2018, 2019, Luat *et al.* 2020b). However, predictive models derived from the MARS algorithm, as well as the other machine learning techniques, have never been implemented for shallow foundation settlement problems.

In order to implement a MARS model, users need to select tuning hyperparameters which include the maximum number of terms  $M_{max}$ , maximum interaction between variables  $I_{max}$ , and penalty  $d$ . These hyperparameters are considered as essential features governing MARS model complexity and generalization. Therefore, obtaining an optimal model is essential to achieve MARS prediction accuracy. Friedman's recommendations for selecting hyperparameters have large value ranges, with actual hand-picked values reliant on the dataset we are dealing with. Due to this drawback, other searching engines have been developed to solve the optimization problem.

A survey of the published literature shows that a number of nature-inspired algorithm have been increasingly developed to optimize hyperparameters of machine learning models such as Artificial bee colony (ABC) (Cheng and Cao 2014), Balancing composite motion optimization (Le-Duc *et al.* 2020), Firefly algorithm (FA) (Bui *et al.* 2018), and Genetic algorithm (GA) (Gomes *et al.* 2019), *etc.* In this study, the Genetic Algorithm (GA) was utilized as an evolutionary search engine to obtain optimal MARS hyperparameter values. This combination was considered as a hybrid intelligent technique, namely GA-MARS. GA was first popularized by Holland (1975) and further developed by Goldberg (1989). Notably, GA is a powerful technique to find global optima values in complex search space (multi-modal, multi-objective, non-linear, discontinuous, and highly constrained space). Because of this capability, GA has gained popularity in several engineering fields (Gesoglu and Güneysi 2007, Gandomi *et al.* 2010, Nehdi and Nikopour 2011, Golafshani *et al.* 2015, Tiachacht *et al.* 2018, Wang *et al.* 2018).

The primary purpose of this research was to develop and verify a hybrid model, GA-MARS. This novel proposed model operates automatically and accurately predicts the settlement of shallow foundation on sandy soil in relation to the bread of foundation ( $B$ ), length to width ( $L/B$ ), the embedment ratio  $D_f/B$ , the net-applied load pressure at footing base ( $q_{net}$ ), and the average SPT blow count ( $N$ ). The second objective is to propose an explicit prediction formula interms of the above variables. To do these things, a database contained 180 experimental data reported by Luat *et al.* (2020a) was used for training and testing model. The GA-MARS performance were then compared against some traditional methods and an ANN model developed by Shahin *et al.* (2002).

## 2. Overview of empirical methods and ANN model

A review of related researches is given in this section for the sake of comparison with this study. Three empirical

methods performed by Schultze and Sherif (1973), Meyerhof (1974), Anagnostopoulos *et al.* (1991) and an ANN model developed by Shahin *et al.* (2002) were chosen to compare and assess the reliability of the GA-MARS' performance. These method were chosen since all of which used data from SPT, and the GA-MARS model had similar input variables.

### 2.1 Schultze and Sherif (1973)

From the results of measured settlement at 48 sites with SPT, Schultze and Sherif (1973) suggested an analytical method for estimating settlement of shallow foundations on sand. This settlement can be predicted from:

$$S_c = \frac{q_{net} F_c}{N^{0.87} \left(1 + 0.4 \frac{D_f}{B}\right)} \quad (1)$$

### 2.2 Meyerhof (1974)

Meyerhof's most recent expressions for settlement were further modifications of his previous methods (Meyerhof 1974) and were generally considered to be conservative. In this case, when the base embedment was considered, the settlement was as follows:

$$S_c = \frac{1.33q_{net}}{N} \left(1 - \frac{D_f}{B}\right) \text{ for } B \leq 1.22 \text{ m} \quad (2)$$

$$S_c = \frac{0.53q_{net}}{N} \left(\frac{2B}{B + 0.3}\right)^2 \left(1 - \frac{D_f}{4B}\right) \text{ for } B > 1.22 \text{ m} \quad (3)$$

### 2.3 Anagnostopoulos (1991)

Anagnostopoulos *et al.* (1991) suggested another empirical method for grouping estimates according to stiffness, e.g., loose, medium, or dense sand, as well as small versus large footings. This approach was based on a statistical evaluation of measured settlements and multiple case history analyzes obtained primarily from Schultze and Sherif (1973) and Burland and Burbidge (1985). Appropriate expression for both SPT blow count range and footing width would presumably be used to estimate settlement. Then, on average, these two results give a single estimate of settlement. Such predicting settlement formulae can be expressed as:

$$S_c = (0.57q^{0.94}B^{0.90})/N^{0.87} \text{ for } 0 < N \leq 10 \quad (4)$$

$$S_c = (0.35q^{1.01}B^{0.69})/N^{0.94} \text{ for } 10 < N \leq 30 \quad (5)$$

$$S_c = (604q^{0.90}B^{0.76})/N^{2.82} \text{ for } N > 30 \quad (6)$$

$$S_c = (1.90q^{0.77}B^{0.45})/N^{1.08} \text{ for } B \leq 3 \text{ m} \quad (7)$$

$$S_c = (1.64q^{1.02}B^{0.59})/N^{1.37} \text{ for } B > 3 \text{ m} \quad (8)$$

### 2.4 ANN model

Shahin *et al.* (2002) successfully applied ANN for

settlement prediction of shallow foundations on granular soils. The optimal ANN structure was found to be 5-2-1 (five input variables, one hidden layer with two neurons, and an output neuron). In a further development, a design formula was derived as follows:

$$S_c = 0.6 + \frac{120.4}{1 + e^{(0.312 - 0.725 \tanh x_1 + 2.984 \tanh x_2)}} \quad (9)$$

and

$$x_1 = 0.1 + 10^{-3} \left[3.8B + 0.7q + 4.1N - 1.8 \frac{L}{B} + 19 \frac{D_f}{B}\right] \quad (9a)$$

$$x_2 = 10^{-3} \left[0.7 - 41B - 1.6q + 75N - 52 \frac{L}{B} + 740 \frac{D_f}{B}\right] \quad (9b)$$

where, in Eq. (1-9),  $S_c$  = settlement (mm);  $q_{net}$  = net applied pressure (kPa);  $B$  = footing width (m);  $D_f$  = depth of embedment (m);  $N$  = the blow count from SPT, were not corrected for overburden stress;  $\sigma'_c$  = pre-consolidation pressure (kPa); and  $F_c$  = settlement coefficient (obtained from design chart).

## 3. Methodology

### 3.1 Multivariate adaptive regression splines (MARS)

Multivariate adaptive regression splines was first introduced by Friedman (1991), as a procedure for adaptive nonlinear and nonparametric regression that makes no assumption about the underlying functional relationship between the predictors and the target outputs. The general expression of nonparametric regression can be represented as:

$$y_i = f(x_{i1}, x_{i2}, \dots, x_{ij}) = f(X) + \varepsilon_i \quad (10)$$

in which  $X = (x_{i1}, x_{i2}, \dots, x_{ij})$  is an  $i \times j$  matrix of  $j$  input features and  $i$  samples and  $\varepsilon_i$  is the error distribution of the  $i$ th sample, also called noise. The main goal of this regression is to estimate the general function of high dimensional arguments  $f(x_{i1}, x_{i2}, \dots, x_{ij})$  directly, rather than to estimate parameters. For this purpose, it is assumed that  $f(X)$  is a smooth, and continuous function.

A MARS model is established by applying basis functions (known as terms) to approximate the function

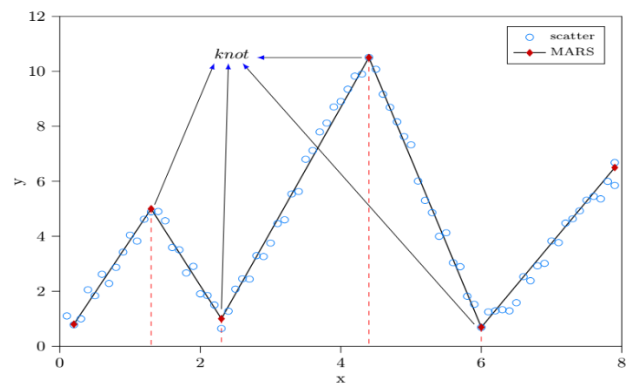


Fig. 2 A simple example of linear splines and knots

$f(X)$ . Basis functions are splines (also called smooth polynomials), which have pieces, including piece-wise linear and piece-wise cubic functions that connect smoothly together. However, only the piece-wise linear function is expressed for simplicity. The interface points between the linear piece-wises are called knots illustrated as solid markers in Fig. 2 and denoted  $t$ . The knot location separates the spline basis function into two-sided truncated functions, is expressed formally as

$$b_q^-(x-t) = [-(x-t)]_+^q = \begin{cases} (t-x)^q & \text{if } x < t \\ 0 & \text{otherwise} \end{cases} \quad (11)$$

$$b_q^+(x-t) = [+(x-t)]_+^q = \begin{cases} (x-t)^q & \text{if } x > t \\ 0 & \text{otherwise} \end{cases} \quad (12)$$

where  $t$  is the knot location,  $b_q^-(x-t)$  and  $b_q^+(x-t)$  are the spline functions, the  $[\ ]_+$  ensures these values are positive, and the power  $q$  equals to 1 for simplicity as mentioned above.

The general form of the MARS model for predicting output  $\hat{y}$  can be expressed as

$$\hat{y} = f(X) = c_0 + \sum_{m=1}^M c_m B_m(x) \quad (13)$$

where  $x$  is the input variable;  $c_0$  is a constant;  $B_m(x)$  is the  $m^{th}$  basis function; and  $c_m$  is the coefficient of  $B_m(x)$ .

In general, MARS contains the following three steps: (i) the constructive phase: a forward stepwise algorithm to select certain spline basis functions, (ii) the pruning phase: a backward stepwise algorithm to delete unnecessary basis functions until the “best” set is found, and (iii) optimum model selection. The constructive phase first starts on the training data with only the intercept,  $c_0$ , and then several knots are created automatically. These knots are points at random locations within the range of each input variables to define a pair of basis functions. At each step, the model adopts the knot and its corresponding pair of basis function that produces the most significant decrease in the residual sum of squares error. Considering a current model with several basis functions ( $M$ ), the next pairs are added to the model in the form

$$c_{m+1} B_m(X) [+(x-t)]_+^q + c_{m+2} B_m(X) [-(x-t)]_+^q \quad (14)$$

This process continues until the maximum number of terms  $M_{max}$  is reached. The value of  $M_{max}$  should be chosen larger than the optimal model size as referenced Friedman (1991). Typically, the basis functions addition leads to a very complicated and overfit model. In the second phase, a backward deletion is employed to overcome this problem. The aim of this phase is to find an optimal model by removing redundant basis functions and irrelevant variables as well. Friedman (1991) also recommended the generalized cross-validation (GCV) originally proposed by Craven and Wahba (1978) as a deletion criterion. The value of GCV is defined as follows:

$$GCV = \frac{1}{n} \times \frac{\sum_{m=1}^M (y_i - \hat{y}_i)}{(1 - C(M)/n)^2} \quad (15)$$

where  $n$  is the number of data sets,  $y_i$  is the response value

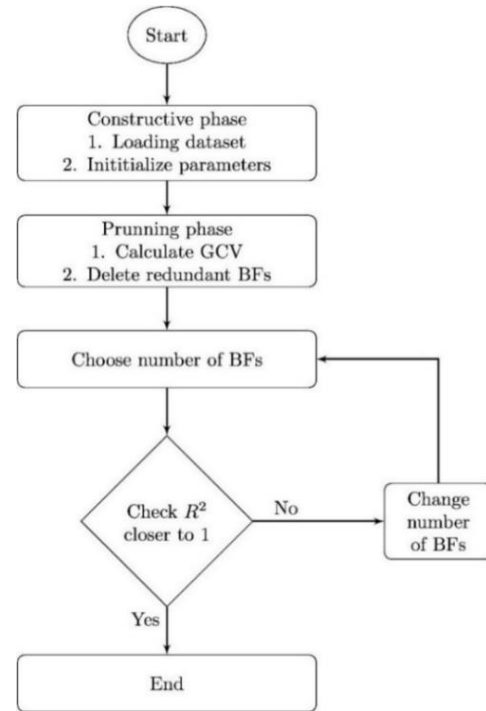


Fig. 3 The flowchart of the MARS model

of the  $i^{th}$  data,  $\hat{y}_i$  is the predicted values obtained from the MARS model of the  $i^{th}$  data, and  $C(M)$  is a penalty factor that increases with the number of terms that can be determined as

$$C(M) = M + dM \quad (16)$$

where  $d$  is a penalty factor for each basis function optimization and is a smoothing parameter. Friedman (1991) provided more details about the selection of  $d$ . At each backward step, a basis function is removed to minimize Eq. (15), until an adequately fitting model is found. Finally, in the third phase, the best MARS model is selected. The flowchart of the MARS model is shown in Fig. 3.

An analysis of variance (ANOVA) decomposition of the MARS model can be used to assess the contributions from the input variables and the basis functions. This procedure groups together all the basis functions that involve one variable and another grouping of terms that involve pairwise interactions. ANOVA function for MARS model is given by the following expression:

$$f(x) = \beta_0 + \sum_{B=1} f_i x_i + \sum_{B=2} f_{ij} x_{ij} + \sum_{B=3} f_{ijk} x_{ijk} + \dots \quad (17)$$

where  $\sum_{B=1} f_i x_i$  is the total basis functions that involve only a single variable,  $\sum_{B=2} f_{ij} x_{ij}$  is total basis functions that involve exactly two variables and  $\sum_{B=3} f_{ijk} x_{ijk}$  represents the contributions from three variables interactions (if present).

### 3.2 Genetic algorithm (GA)

In general, an individual is characterized by a set of

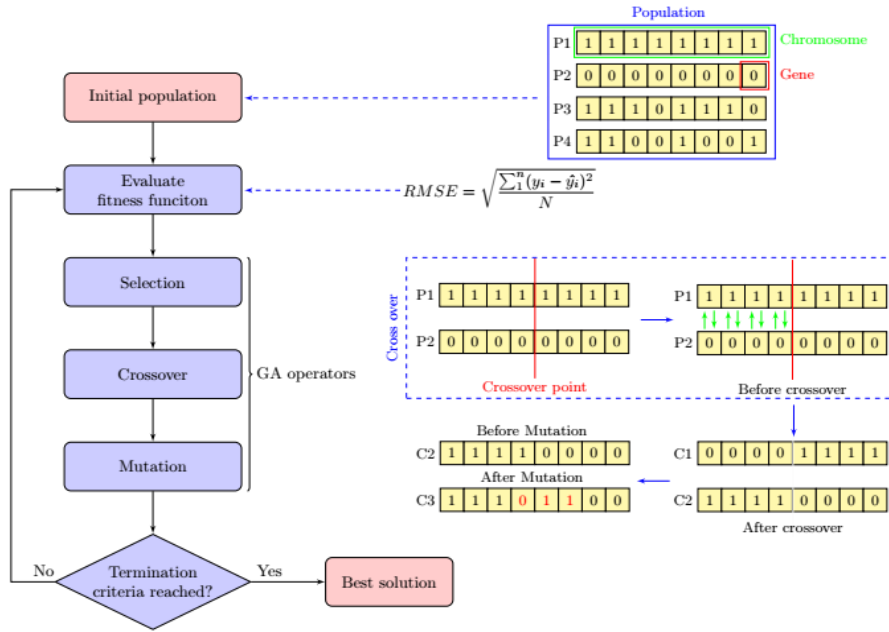


Fig. 4 The GA flowchart

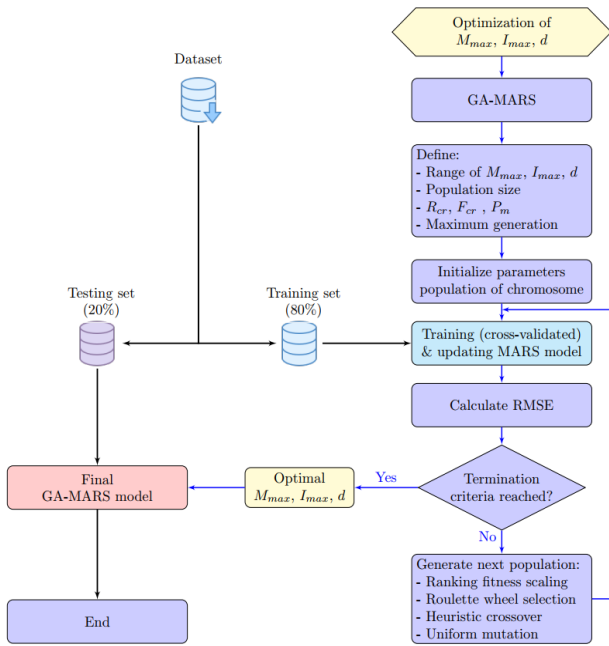


Fig. 5 The GA-MARS procedure

parameters (variables), as called genes. Genes are joined into a string to form a chromosome. In GA, a chromosome has a fixed length that encodes genes to binary values (a string of 0s and 1s). The implementation of GA may be specified in the following steps: (i) population initialization; (ii) evaluate fitness function; (iii) selection; (iv) crossover and mutation; (v) termination.

Commonly, the GA starts with a set of individuals is randomly generated, called initial population. Then, the adaptation of each individual is estimated by the fitness function, e.g., root mean square error (*RMSE*), which determines the ability of an individual to contend with the others. Each individual is given a fitness score as a basis of the selection for reproduction. The GA then selects two

pairs of individuals (parents) according to their fitness score (the higher fitness score is, the more chance they are to be selected). Crossover is the most significant phase in GA, where the parents pass their genes to the next generation. A crossover point is randomly chosen to determine the range of genetic exchange between two parents. When the genetic exchange of parents among themselves reaches the crossover point, a new individual, as called child, is created and added to the population. The child returned can be expressed as:

$$C = P2 + R_{cr} \times (P1 - P2) \quad (18)$$

where  $R_{cr}$  is the ratio indicating how far the child ( $C$ ) is from the better parent ( $P1, P2$ ), and  $P1 -$  denotes the parent having better fitness value. In addition, the fraction of individuals in the next generation is represented by a parameter  $F_{cr}$ , which has a significant effect on GA performance.

In some newly formed individuals, some of their genes may be mutated with low random probability,  $P_{mut}$ . Mutation adds to the diversity of a population and thereby increases the likelihood that GA generates better individuals. It occurs to maintain variety within the population and prevent premature convergence. Finally, the GA terminates if the stopping condition is satisfied, and the best solution is found in the current population. This condition can be based on the chromosome structure or the special meaning of the chromosome. The former governs the number of genes that are converging, whereas the latter examines the algorithm evolution after each generation. The GA finishes if the number of genes is equal or higher than an identical value, or its change is less than a constant. When the stopping conditions are not met, this process is repeated with the new population until creating the best generation. The executable GA is graphically illustrated in Fig. 4.

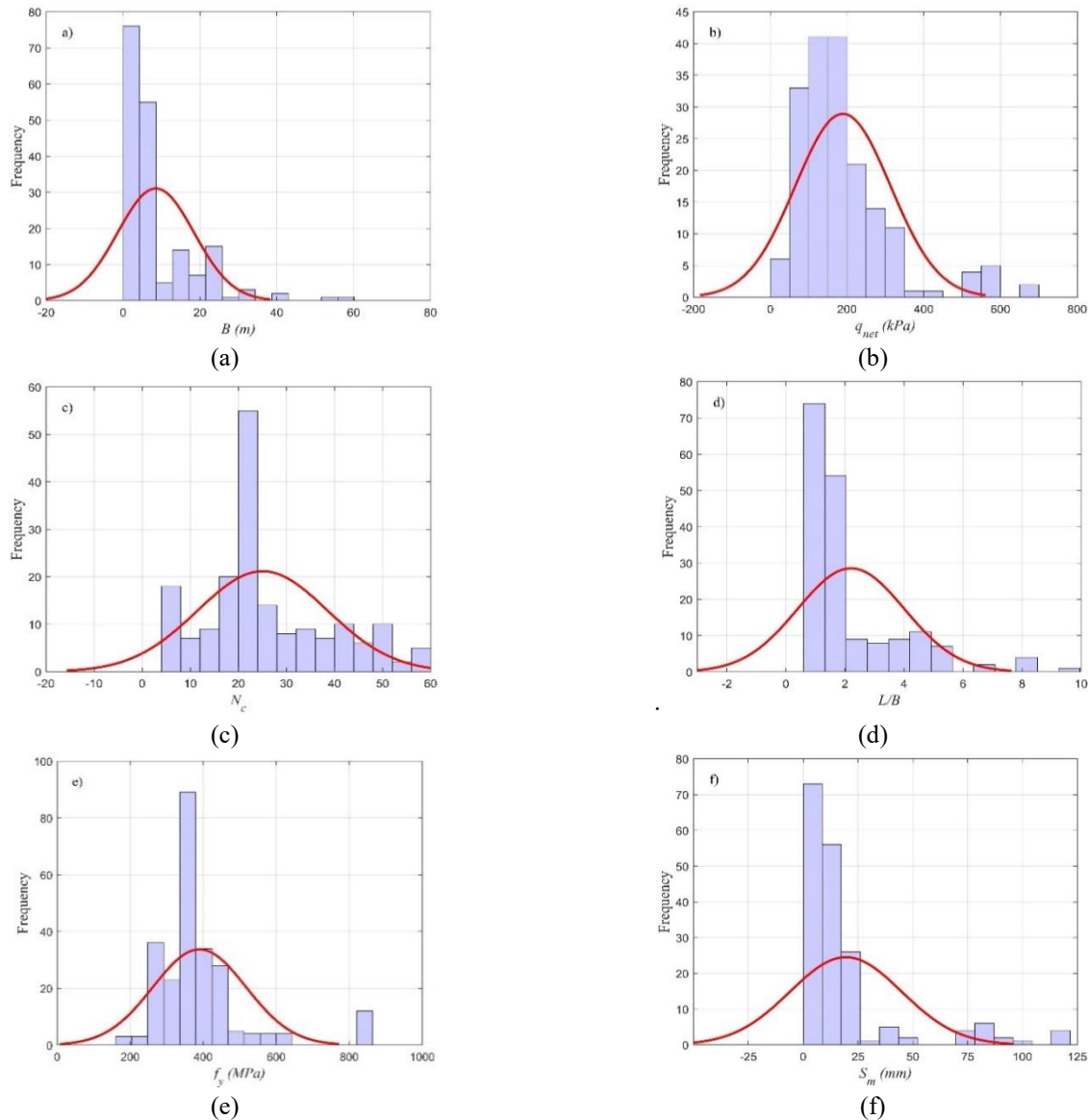


Fig. 6 Histogram of dataset distribution. (a) Width of foundation, (b) Net-applied pressure, (c) SPT blow count, (d) Length to width ratio, (e) Embedment ratio and (f) Measured settlement

### 3.3 Hybrid model

In engineering applications, many kinds of researches have been carried out to finding the optimal values of hyperparameters of a machine learning model (Bui *et al.* 2018, 2019, Qi and Tang 2018, Iyer *et al.* 2019, Pramanik and Maiti 2019). In this study, a hybrid system GA-MARS is implemented to predict the settlement of shallow foundation on sandy soil. In this proposed system, three hyperparameters of MARS, i.e.,  $M_{max}$ ,  $I_{max}$ , and  $d$ , are considered and searched the global optima by GA. The root mean square error (*RMSE*) was adopted as the objective function for the optimization process. The GA-MARS model is depicted in Fig. 5. Further detail of implementation would be discussed later.

## 4. Database description

The experimental data used in this study consisting of

Table 1 Summary of input settings and outputs

Description	Notation	MARS Parameters	Min.	Max.	Mean	Std.
Breadth of foundation (m)	$B$	$X_1$	0.8	255	9.82	20.48
Length to width	$L/B$	$X_2$	1	10.6	2.19	1.8
Embedment ratio	$D_f/B$	$X_3$	0	3.44	0.53	0.58
Net-applied pressure (kPa)	$q_{net}$	$X_4$	18.32	1532	194.31	157.35
SPT blow count	$N_c$	$X_5$	4	60	24.58	13.53
Measured settlement (mm)	$S_c$	$y$	3.3	103.4	20.2	26.1

180 SPT-based case histories reported in previous research

(Luat *et al.* 2020a). It should be noted that some outliers were removed before training. The input variables used to predict the settlement of shallow foundation consist of the breadth of the foundation ( $B$ ), length to width ( $L/B$ ), the embedment ratio ( $D_f/B$ ), the net-applied pressure at footing base ( $q_{net}$ ), and the average SPT blow count ( $N$ ). The measured settlement of a shallow foundation ( $S_c$ ) is used as the output variable. The ranges of considered variables in this study are summarized in Table 1, and the distribution of each input variable is illustrated in Fig. 6.

It is noteworthy that the uncorrected N-values were used in predicting settlement, however, if the sand was dense, saturated and very fine or silty, Terzaghi and Peck (1968) recommended that the blow count applied to any submerged case should be corrected according to:

$$N_c = 15 + 0.5(N - 15) \quad (19)$$

If the soil was gravelly sand or sandy gravel, a correction for  $N$  was recommended by Burland and Burbidge (1985) as:

$$N_c = 1.25N \quad (20)$$

## 5. Developed GA-MARS model

### 5.1 Checking and preprocessing data

The Pearson correlation coefficient between any two input variables was calculated, as shown in Fig. 7. The correlations between five input variables are not significant, with the maximum value of 0.4 between  $q_{net}$  and  $N_c$ , indicating that the input selection is reasonable.

Due to the difference in dimensions and magnitude orders between the input and output variables, it is necessary to convert them to the same order of magnitude without dimension. Therefore, all of the original input parameters were normalized, making the data 0 mean and 1 standard deviation before training. This rescaling was done to make training less sensitive to the scale of the input variables and to eliminate their dimensions. Moreover, normalization makes the problem better conditioned and improves the convergence rate of the gradient descent. In this research, all variables were normalized using the min-max normalization method, which is expressed as follows:

$$x_{norm} = \frac{x - \min(x)}{\max(x) - \min(x)} \quad (21)$$

where,  $x$  is the original value and  $x_{norm}$  is the normalized value.

### 5.2 Hybrid model development

The interpreted high-level programming language, Python, with its implementation called *py-earth* package, was used for the development of the MARS model. As mentioned above, one may construct a MARS model with a variety of hyperparameter options, including a maximum basis function (max terms)  $M_{max}$ , maximum interaction (also called as product degree)  $I_{max}$ , and penalty parameter  $d$ . However, while setting the optimal parameters

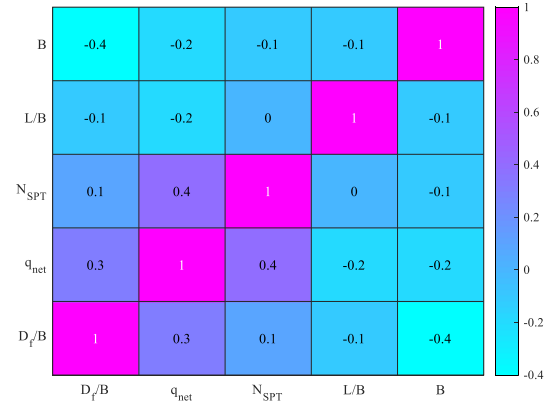


Fig. 7 Correlation matrix of five input

simultaneously is difficult using MARS, such optimization significantly improves the prediction accuracy of MARS. A hybrid model GA-MARS was developed thus utilized to overcome this problem, illustrated in Fig. 5. The step involved are summarized below:

#### i) Initializing and encoding

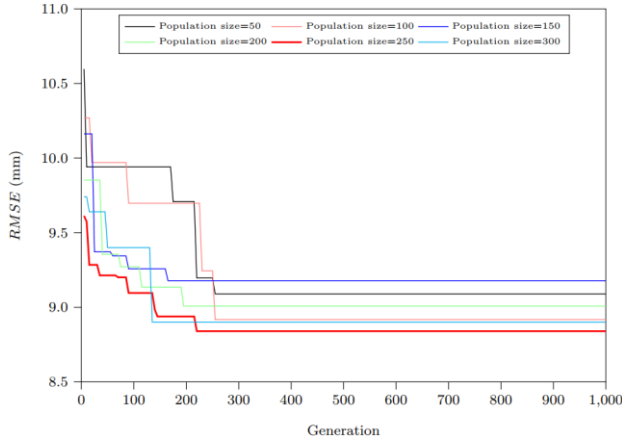
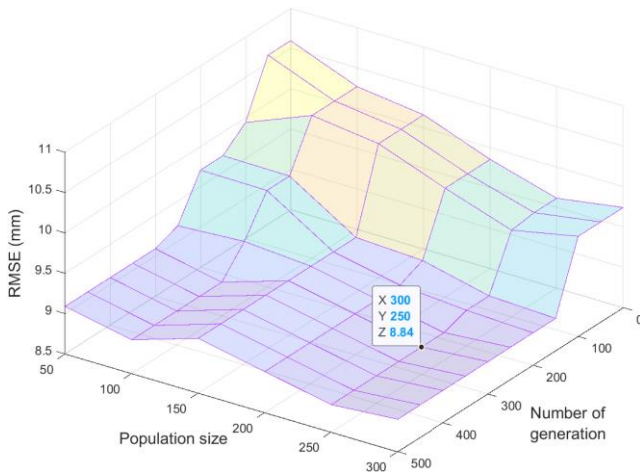
Three MARS hyperparameters to be optimized were encoded in binary format to produce the chromosomes. Elements of the chromosome  $P$  defined by  $P\{p_1, p_2, p_3\}$  represented  $(M_{max}, I_{max}, d)$  where,  $p_1$  and  $p_2$  were integer values, and  $p_3$  was a continuous value. The  $k$ -fold cross-validation method was used in this research to reduce the over-fitting problem in the selected model. With 175 experimental data (after removing outliers), the 10-fold was chosen for developing the hybrid model. Firstly, the whole data was divided into two partitions, namely training set with 140 cases (80%) and testing set with 35 cases (20%). To implement the cross-validated procedure, the training data were randomly selected and split into 10 distinct folds, which mean each fold contains 14 cases (10% of 140). For each iteration, MARS model was performed on a training subset (nine of ten folds) using a specific combination of  $(M_{max}, I_{max}, d)$ , while the remaining one dataset was used to validate model performance by calculating the fitness value from fitness function. The 10-fold cross-validation technique strategy is presented in Fig. 8. This procedure is repeated for each fold in the training set so that all folds were used once as the validation fold. In this case, the fitness function was the root mean square error ( $RMSE$ ), defined below

$$RMSE = \sqrt{\frac{1}{n} \times \sum_{i=1}^n (y_i - \hat{y}_i)^2} \quad (22)$$

where  $n$  is the sample number in the training set, a chromosome with the lowest values of  $RMSE$  has the highest probability of surviving in the next generation.

#### ii) GA operators

The previous population was replaced by the offspring after completing the GA operators, i.e., selection, crossover, and mutation. The ratio  $R_{cr}$ , the crossover probability  $F_{cr}$ , and mutation probability  $P_{mut}$ , were chosen 1.2, 70%, and 10%, respectively (Ren and Bai 2010, Koopialipoor *et al.*

Fig. 8  $k$ -fold (10-fold) cross-validation schemeFig. 9 The  $RMSE$  curve of GA-MARS model accordance with various population sizesFig. 10 The 3-D surface of GA-MARS performance with various population sizes and generations (X = number of generations; Y = population size; Z =  $RMSE$ )

2019), and defined at the first step. In this stage, GA searches the best combination of hyperparameters ( $M_{max}$ ,  $I_{max}$ ,  $d$ ) in each generation.

### iii) Terminating criteria

The optimization process is stopped once the termination criterion is satisfied. Before reaching this point, the GA-MARS model proceeds to the next generation. Because GA was used as an evolutionary search engine, the stopping criterion is often the maximum number of generations ( $G_{max}$ ) and the repetition of the optimum for a determined number of generations. If this occurs, it is assumed that the algorithm has already converged.

### iv) Estimating model and decoding parameters

The best MARS model with optimal parameter settings

Table 2 The hybrid GA-MARS model parameters

Component	Program parameter	Setting
<b>MARS model</b>		
Estimator type	estimator	earth()
Evaluation	scoring	r2
Maximum number of basis function ( $M_{max}$ )	max_term	(1; 50)
Maximum interaction of terms ( $I_{max}$ )	max_degree	(1; 9)
Smoothing parameter ( $d$ )	penalty	(2; 4)
Number of extreme data values of each feature not eligible as knot locations	end_span	
Parameter controlling end_span	endspan_alpha	(0; 1)
Parameter controlling endspan_alpha	minspan_alpha	(0; 1)
Kind of feature importance	feature_importance_type	GCV
Cross-validation method	K-fold	-
Number of folds	n_splits	10
Training partition		80%
Testing partition		20%
<b>Genetic algorithm</b>		
Maximum generation	$G_{max}$	300
Population size	$P_s$	250
Combinatorial variables		
- $M_{max}$	P1	integer
- $I_{max}$	P2	integer
- $d$	P3	float
Differential ratio	$R_{cr}$	1.2
Crossover ratio	$F_{cr}$	0.7
Mutation ratio	$P_{mut}$	0.1
Fitness function	$RMSE$	-

was obtained when the termination criterion was fulfilled. It means that GA-MARS has completed the training process and is active in predicting new input data (testing set). However, all the encoded parameters need to be decoded following:

$$X_{dec} = p \sum_{i=1}^{L_c} bit \times 2^i + b_{lower} \quad (23)$$

where,  $X_{dec}$  – decoding value;  $p$  – precision is calculated as:  $p = \frac{b_{upper} - b_{lower}}{2^{L_c} - 1}$ , in which  $b_{upper}$  and  $b_{lower}$  are upper bound and lower bound of parameter  $X$ , respectively;  $L_c$  is the chromosome length;  $bit$  is a binary value (0 or 1).

A parametric study was employed for determining the maximum number of generation ( $G_{max}$ ) and population size ( $P_s$ ), which affect significantly hybrid system performance. To obtain the best of  $G_{max}$ , a value of 1000 generation was assigned as stopping criteria calculating  $RMSE$ . In further analysis, a series of hybrid GA-MARS models were investigated to determine the best population size (among values of 50, 100, 150, 200, 250, 300). Fig. 9 shows that the  $RMSE$  values are unchanged after generation 300<sup>th</sup>. With

Table 3 Cross-validation GA-MARS training and testing results

Fold	Training			Testing			Hyperparameter		
	<i>MAE</i>	<i>RMSE</i>	$R^2$	<i>MAE</i>	<i>RMSE</i>	$R^2$	$M_{max}$	$I_{max}$	$d$
	(mm)	(mm)		(mm)	(mm)				
1	3.32	5.15	0.985	3.51	6.12	0.966	23	2	4.01
2	4.64	6.33	0.949	4.87	7.09	0.932	11	1	3.28
3	4.78	6.54	0.954	4.97	6.95	0.937	18	4	2.02
4	4.79	6.34	0.955	4.95	6.88	0.94	35	4	2.72
5	3.18	5.06	0.991	3.34	5.59	0.971	13	4	2.17
6	3.68	6.41	0.981	4.08	6.32	0.963	33	4	3.31
7	4.2	6.12	0.968	4.46	6.62	0.949	24	3	2.4
8	3.8	5.6	0.971	4.1	6.51	0.953	13	2	1.6
9	3.06	4.83	0.99	3.46	5.65	0.97	19	2	2.76
10	3.21	6.36	0.985	3.5	6.36	0.959	21	3	3.47
Avg.	3.87	5.87	0.973	4.12	6.41	0.954			
Std.	0.65	0.61	0.015	0.62	0.49	0.013			

further depiction in Fig. 10, it is clear that the population size of 250 can provide stable performance with gradually decreasing and lowest value of *RMSE*. Therefore, the optimal generation and population size chosen in this study were 300 and 250, respectively.

Beside using *RMSE* as the fitness function, the performance of the proposed GA-MARS model was evaluated by other following criteria indices:

- Coefficient of determination ( $R^2$ ):

$$R^2 = 1 - \frac{\sum_{i=1}^n (y_i - \hat{y}_i)^2}{\sum_{i=1}^n (y_i - \bar{y}_i)^2} \quad (24)$$

- Mean Absolute Error (*MAE*):

$$MAE = \frac{1}{n} \sum_{i=1}^n |y_i - \hat{y}_i| \quad (25)$$

where  $y$  is the actual values;  $\hat{y}_i$  is the predicted value;  $\bar{y}_i$  is the mean of the actual values; and  $n$  is the number of samples. For a prediction model with high accuracy,  $R^2$  should be close to 1, which is the maximum value.

The selection of MARS model parameters were based on the following:

Scoring evaluation was coefficient of determination ( $R^2$ ).

- The training and testing partition size was 80% and 20%, respectively.
- The size of validation was 20% of training set.
- The maximum number of basis function for training was in the range of 1 and 50.
- The maximum interaction of terms was from 1 to 9.
- The penalizing parameter was in the range of 2 and 4, with a default value of 3.
- The number extreme data values of each feature not eligible as knot locations was a default value of -1.
- The parameter controlling “endspan” was randomly chosen the range of 0 to 1.
- The parameter controlling “mindspan” was randomly

chosen in the range of 0 to 1.

- The feature importance criterion was GCV.

To sum up, all parameters for the proposed GA-MARS model are listed in Table 2.

### 5.3 GA-MARS performance

This study evaluated the model efficiency using the K-fold method with a stratified 10-fold cross-validation. Random selection divided the 140 of training data into 10 distinct folds. Each fold was employed in turn as validating data, with the remaining folds used as training data, ensuring that all cases in training set were applied in both the training and validating phases.

Table 3 demonstrates the performance of the GA-MARS model in predicting the settlement of shallow foundations on sandy soils over 10 folds. As shown in this table, the GA-MARS model attains outstanding average  $R^2$  values (close to 1) for both training ( $R^2 = 0.973$ ) and testing data ( $R^2 = 0.954$ ), indicating that the model accurately estimates the underlying function of the settlement of shallow foundations. In terms of *MSE* and *RMSE*, the proposed model yielded small average values for both training and testing data. The *MSE* values obtained of 3.87 and 4.12 mm, for training and testing set, while the *RMSE* values were 5.90 and 6.41 mm, respectively. The low standard deviation values between two sets (6.1% of *MSE*, and 7.8% of *RMSE*) illustrated stable model generalizability.

The hyperparameter configuration of the GA-MARS model is also given in Table 3. Remarkably, the values of maximum basis function  $M_{max}$  which varied in the range from 11 to 35, affect the accuracy of prediction significantly. Also, the number of interactions among input variables  $I_{max}$  alternated between 1 and 4. It was found that no fold had a default value of penalty parameter  $d$  within the referred range (Friedman 1991). Therefore, it can be concluded that simultaneously choosing suitable parameter values is a challenge for users. This statement coincides

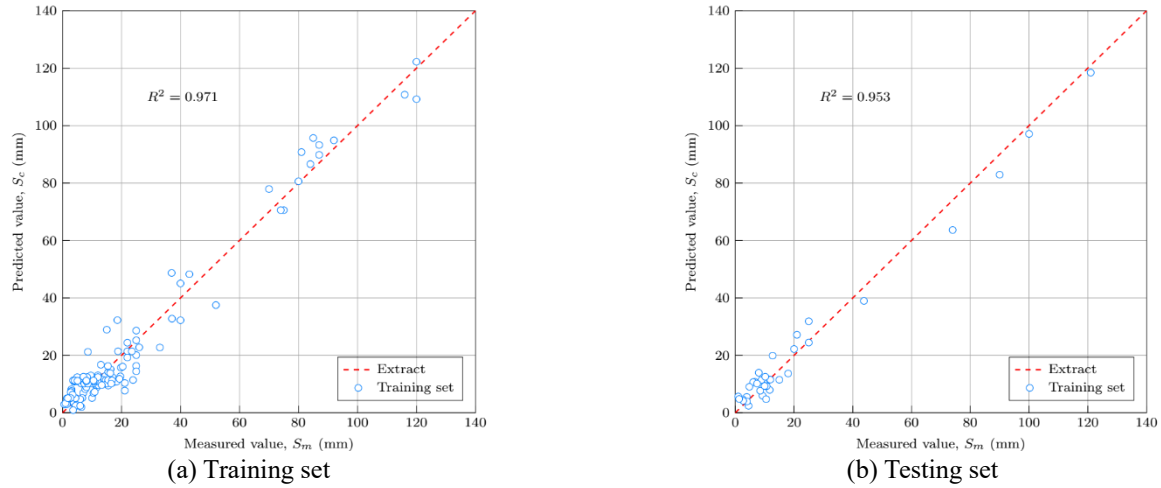


Fig. 11 The correlation between predicted and actual output performing on fold 8

Table 4 Basis function of the MARS model with the corresponding equation and coefficients

$B_m(x)$	Equation	$(c_m)$
$B_0(x)$	1	10.682
$B_1(x)$	$\max(0, 4 - B)$	3.760
$B_2(x)$	$\max(0, B - 4)$	0.286
$B_3(x)$	$\max(0, 12 - N_c)$	3.642
$B_4(x)$	$q_{net} \times \max(0, 12 - N_c)$	0.028
$B_5(x)$	$\max(0, B - 4) \times \max(0, 116.8 - q_{net})$	-0.025
$B_6(x)$	$\max(0, 4 - B) \times \max(0, N_c - 18)$	-2.772
$B_7(x)$	$\max(0, 4 - B) \times \max(0, 18 - N_c)$	-1.652
$B_8(x)$	$\max(0, 4 - B) \times \max(0, N_c - 20)$	2.734
$B_9(x)$	$\max(0, B - 4) \times \max(0, 24 - N_c)$	0.151
$B_{10}(x)$	$\max(0, B - 4) \times \max(0, 0.13 - D_f/B)$	8.211

Table 5 Results of ANOVA decomposition

Function	GCV	# $B_m(x)$	Variable(x)
1	188.41	2	$B$
2	64.49	1	$N_c$
3	220.92	4	$B, N_c$
4	55.85	1	$q_{net}, N_c$
5	54.18	1	$B, q_{net}$
6	61.72	1	$B, D_f/B$

Table 6 Comparison of MARS model and available method

Method	$MAE$	$RMSE$	$R^2$
	(mm)	(mm)	
Schultze and Sherif (1973)	14.58	29.01	0.104
Meyerhof (1974)	11.95	26.43	0.444
Anagnostopoulos <i>et al.</i> (1991)	7.9	15	0.768
ANN – Shahin <i>et al.</i> (2002)	8.78	11.04	0.819
GA-MARS (This study)	4.12	6.41	0.954

with Cheng and Cao's investigation (Cheng and Cao 2014). However, it should be noted that the instance of these

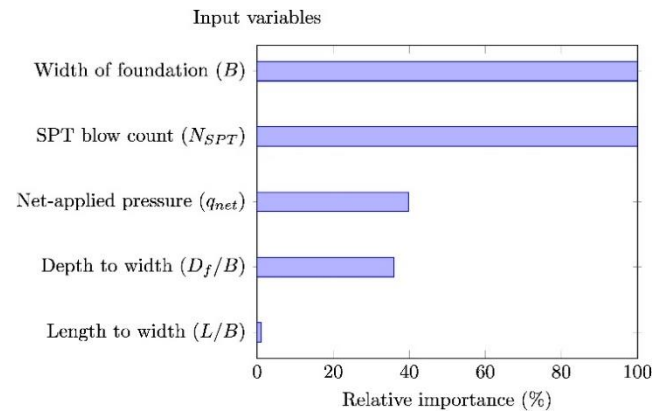


Fig. 12 The relative importance of input variables

parameter values depends on user experience and may be beyond the suggested range.

Fold 8 was chosen to derive the MARS formulation as its findings were close to the average values. Table 4 presents the basis functions of the MARS model with corresponding equations and coefficients ( $c_m$ ). As four out of five input variables were used to approximate functions, the one-remaining variable was ignored without influencing the estimated results. It is noteworthy that all input parameters were normalized using Eq. (15). Hence, the variables of the basis functions in Table 4 were rescaled before deriving corresponding equations. Finally, the settlement of shallow foundation on sandy soil  $S_c$  was expressed by the MARS model as

$$\begin{aligned}
 S_c = & 10.682 + 3.760 \times B_1(x) + 0.0286 \times B_2(x) \\
 & + 3.642 \times B_3(x) + 0.028 \times B_4(x) \\
 & - 0.025 \times B_5(x) - 2.773 \times B_6(x) \quad (26) \\
 & - 1.652 \times B_7(x) + 2.734 \times B_8(x) \\
 & + 0.151 \times B_9(x) + 8.211 \times B_{10}(x)
 \end{aligned}$$

Fig. 11 graphically shows the correlation between the predicted value and measured value for fold 8 and the correspondence test set. As seen in this figure, the MARS model performs reasonably well for both training

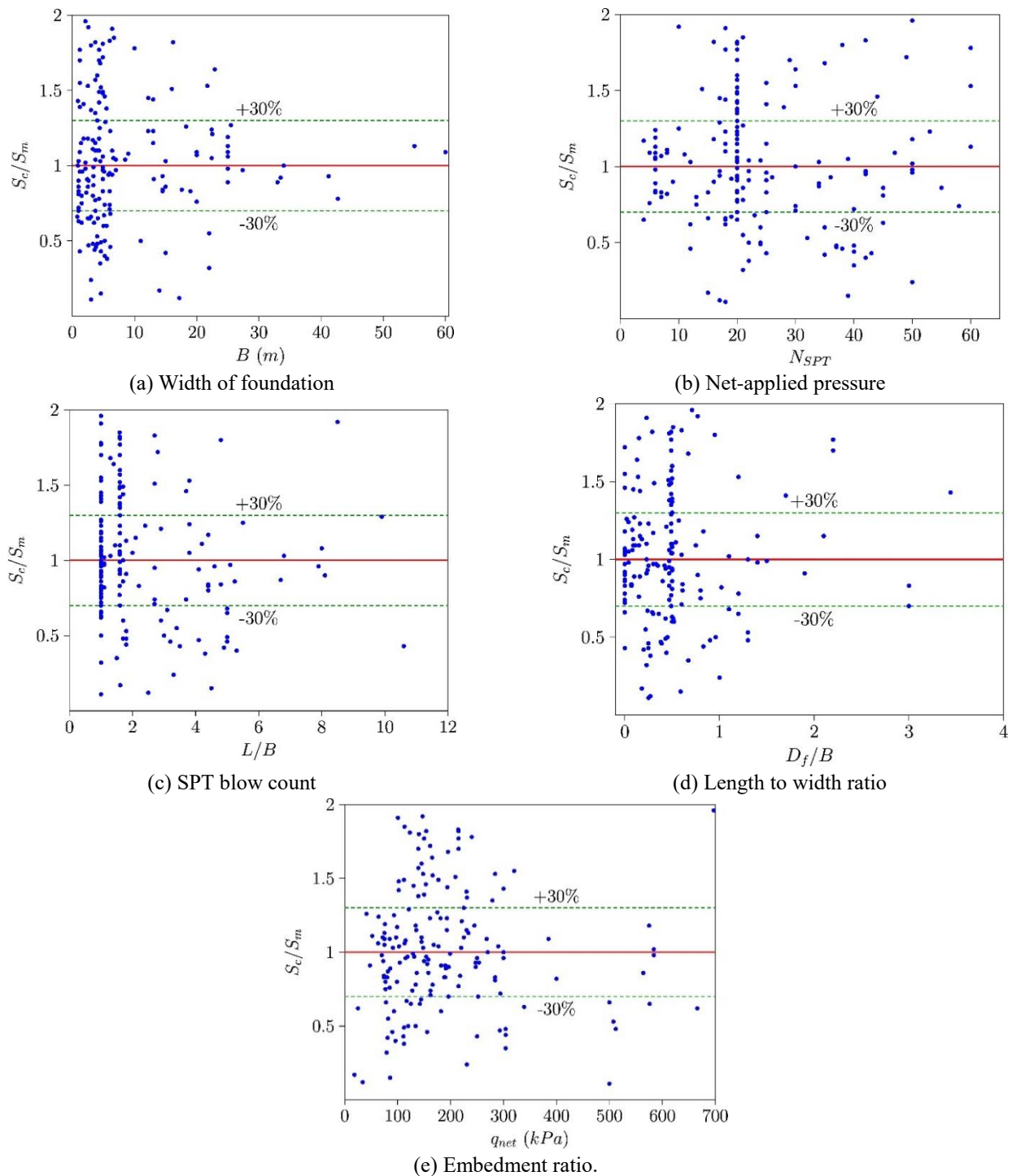


Fig. 13 The ratio of predicted/measured results versus input variables

and testing data, with almost scattering around the best fit line.

As mentioned above, one of the most critical advantages of MARS is its ability to inspect the importance of the input variables based on ANOVA decomposition. Table 5 shows the ANOVA decomposition of the proposed MARS model for fold 8. The GCV column indicates the significance of the corresponding ANOVA functions via the GCV score for a model with all related basis functions to that specific ANOVA function eliminated. This GCV value is used to evaluate whether the ANOVA function contributes

substantially to the model, or marginally increases the global GCV score. The  $\#B_m(x)$  column indicates the number of basis functions in the ANOVA function, and the variable(s) column gives the particular input features related to the ANOVA function.

The final model contained a total of 11 basis functions with a maximum of two degrees of interactions. Fig. 12 indicates the relative importance of the input variables, evaluated by the increase in the GCV value. The two most important variables influencing the prediction were the breadth of foundation ( $B$ ), and the corrected SPT blow

Table 7 Comparison between proposed formula and available formulae in terms of predicted to measured values (performing on testing set)

No.	$B$ (m)	$q_{net}$ (kPa)	$N_{SPR}$	$L/B$	$D_f/B$	$S_{Eq.(1)}/S_m$	$S_{Eq.(2-3)}/S_m$	$S_{Eq.(4-8)}/S_m$	$S_{Eq.(9)}/S_m$	$S_{GA-MARS}/S_m$
1	2.5	70	6	1	0.04	9.2753	7.6190	1.2765	1.1821	1.0215
2	4.9	188	20	1.59	0.47	1.4269	1.4852	1.1172	1.7082	1.3062
3	2.5	158	21	5.24	0	1.1631	1.7882	2.0278	1.0178	1.4722
4	1.5	77	13	1	0.8	0.3726	1.3158	0.5682	0.2669	1.3403
5	6	190	7	1	0	2.3522	4.0473	1.0407	1.1517	1.1625
6	27.4	154	17	1	0	8.4865	3.8343	2.5183	1.3848	1.0297
7	2.5	245	16	1	0	0.5566	0.8261	0.9771	0.6149	0.9677
8	6.4	71.8	18	1.45	0.23	1.3788	1.2617	0.9742	0.6711	0.843
9	1.2	300	50	1	0.42	0.5853	1.3909	2.0735	0.6776	1.0408
10	22.5	221	20	2.9	0.44	1.6822	0.8185	0.5018	0.7122	0.7733
11	33.5	156	19	1	0	8.306	3.4434	2.237	1.1103	1.0856
12	1.2	268	8	1	0.75	0.4179	1.5489	0.6819	0.6795	0.9138
13	33	191	34	1	0.16	5.8281	2.5706	1.2781	3.4617	1.1242
14	4.9	113	20	1.59	0.47	1.4086	1.4661	1.1114	1.1279	0.947
15	1.4	230	25	1	2.1	0.4339	1.3714	0.8039	0.6181	0.7043
16	4.4	93	10	5.5	0.57	0.8701	1.7391	0.4239	0.4041	0.8032
17	1.6	250	25	7.9	0.25	0.748	1.4259	1.6458	0.9772	1.0411
18	3.3	52	8	4.2	0.54	3.1725	7.1205	1.8159	1.0444	0.9005
19	6.1	144.1	23	5	1.1	1.9325	1.8962	1.1685	1.7094	1.0086
20	7	131.2	42	5.1	0.33	2.9474	2.8533	2.3533	1.8818	1.0313
21	3.4	81.4	34	6.7	0	3.1398	4.4069	3.4259	1.644	1.1523
22	4	97	20	1.6	0.5	1.136	1.3067	1.0121	0.8153	0.9128
23	2.4	190	22	1.6	1.9	1.0244	2.2002	1.3386	1.3558	1.1035
24	3	500	18	1	0.25	0.7555	1.0077	1.1709	1.0844	1.0228
25	0.9	300	30	1	1.3	0.3999	1.1357	1.0072	0.6095	1.0137
26	1.2	215	29	1	2.2	0.3386	1.2438	0.6948	0.3978	0.9237
27	3.7	225	20	1.6	0.49	0.5922	0.7085	0.549	0.8351	0.9083
28	14.5	253.5	26	1	0.24	1.4719	0.9378	0.6707	1.6577	1.0791
29	41.2	104	36	1	0.24	2.6456	1.0431	0.505	0.8093	1.0725
30	1.8	575	50	1.6	0.83	0.209	0.4015	0.5697	0.3717	0.8455
31	1.2	150	28	1	0.5	0.2098	0.4603	0.4812	0.2026	0.7161
32	6.1	161	20	1.6	0.49	1.1407	1.063	0.7734	1.1777	0.8126
33	25.5	175	21	1	0.1	2.3336	1.1079	0.7391	0.6709	0.7844
34	1	284	25	2.2	3	0.9462	6.7222	2.1754	1.6351	1.2006
35	18.3	41	20	1	0.02	1.7765	1.0002	0.7237	0.2751	0.7915
Mean						2.0418	2.1305	1.2123	1.0270	0.9959
Standard deviation						2.3246	1.8196	0.7019	0.6171	0.1730

count ( $N_c$ ) was followed sequentially by the net-applied pressure ( $q_{net}$ ) and the depth to width ratio ( $D_f/B$ ). It is clear that the length to width ( $L/B$ ) did not affect the MARS settlement prediction model. This study's two most important variables were identified as highly significant in available studies (Meyerhof 1974), (Anagnostopoulos *et al.* 1991, Anderson *et al.* 2007). Different from the present

study, however, Shahin *et al.* (2002) indicated that the length to width ( $L/B$ ) has the smallest effect on settlement among the five-mentioned input variables, with sensitivity analysis having an average relative important of 9.8. It is elucidated that if two variables are strongly correlated, MARS normally drops one when constructing a model, whereas the ANN model with the lack of theory was unable

Table 8 Comparison between the measured settlement of filed tests and predicted settlement

Experiment No.	Variable					Measured	Method				
	$N$	$B$	$L/B$	$D_f/B$	$q_{net}$		Eq. (1)	Eq. (2)-(3)	Eq. (4)-(8)	Shahin <i>et al.</i> (2002)	This study
1	130	1.82	1.0	0.55	171	1.27	17.01	5.15	9.05	19.75	1.21
2	13	3.0	1.0	0.55	400	11.94	37.17	14.29	24.07	40.63	11.15
3	25	13.1	1.82	0.23	47.6	3.6	2.39	3.57	4.82	8.12	3.54
4	18	14.0	1.61	0.18	18.3	4.2	1.24	2.00	2.79	13.55	4.98

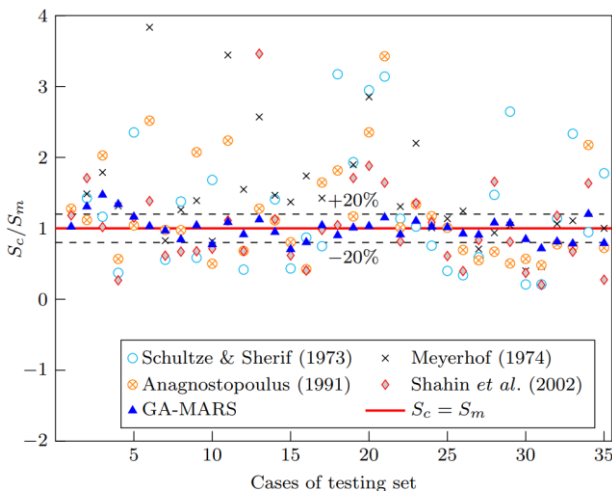


Fig. 14 Measured-to-predicted-settlement ratio of different methods

to remove unnecessary input variables Shahin *et al.* (2002).

For further evaluation, Fig. 13 graphically presents the interaction of input variables with the proposed model. The ratio of predicted value  $S_c$  and measured value ( $S_m$ ) versus five predictors are plotted to illustrate their effectiveness. These plots indicate that even though there are accumulations of data at a specific range of each variable, the predicted values have various scatters that overestimate (above the red solid line), or underestimate (under the solid red line) the settlement. This proves that the generated GA-MARS model does not depend exactly on a particular variable. Therefore, it can be stated that the used predictors are relatively effective in the proposed model, consistent with things shown in the correlation matrix (Fig. 7). It also can be seen in Fig. 13 that only about 25% of data points are outside the margin of  $\pm 30\%$  line (dashed line). By observing Figs. 13(a), and 13(b), it is found that the proposed model can be well-suited for the foundation with more than 10 m widths and the SPT blow count less than 40.

5.4 Results comparison with available methods

To evaluate the proposed MARS model performance, this study compared results with those of three traditional methods, which were introduced above accordance with Eqs. (1)-(9) (Schultze and Sherif 1973, Meyerhof 1974, Anagnostopoulos *et al.* 1991), and an ANN of Shahin *et al.* (2002). Table 6 presents the comparative results in terms of three criteria indices. In terms of *MAE*, the values for testing dataset by Eq. (1), Eq. (2) and (3), Eq. (4) and (8),

ANN and MARS were 14.58, 11.95, 7.90, 8.78, and 4.12. The *RMSE* for the testing set was 29.01, 26.43, 15.00, 11.04, and 6.41, respectively, for the same. Results show that MARS is the fittest model in terms of minimizing *RMSE* values, with a value of nearly 42% below the second-best model (ANN). The methods of Schultze and Sherif (1973), and Meyerhof (1974) achieved the largest *RMSE* values, returning values more than three times greater than the GA-MARS model. The same trend applied to *MAE* values. Moreover, in terms of coefficient of determination ( $R^2$ ) performance, the MARS model attained results that were very close to 1 for the testing set (0.954), while the values are given by Eq. (1), and Eq. (2) and (3) were tiny of 0.1 and 0.443, respectively. These performances prove the proposed model was well-trained for estimating settlement of shallow foundations.

Furthermore, Table 7 shows the predictive performance for the testing set of all considered methods in terms of the ratio of the measured settlement to the predicted settlement. For visualization, this comparison is also depicted in Fig. 14. Almost samples in testing set can be shown to have a variance below  $\pm 20\%$  (points within the two dotted lines) demonstrating the predictability of GA-MARS is superior to the others.

6. Numerical example

A numerical is provided to better explain clearly the implementation of Eq. (26). A square foundation whose dimension is  $14.5 \times 14.5$  m to be constructed overlayer of sand. Given  $D_f = 1$  m; the average SPT blow count is generally increasing with depth and its value in the depth of stress influence = 6. The net applied load on the foundation  $q_{net}$  is 100 kPa.

Solution

From given information,  $D_f/B = 0.5$ , using Eq. (23) with 11 basis function given in Table 4:

- $B_1(x) = \max(0, 4 - B) = \max(0, 4 - 14.5) = 0, c_m^1 = 3.760$
- $B_2(x) = \max(0, B - 4) = \max(0, 14.5 - 4) = 10.5, c_m^2 = 0.286$
- $B_3(x) = \max(0, 12 - N_c) = \max(0, 12 - 6) = 6, c_m^3 = 3.642$
- $B_4(x) = q_{net} \times \max(0, 12 - N_c) = 100 \times \max(0, 12 - 6) = 600, c_m^4 = 0.028$

$$\begin{aligned}
\bullet B_5(x) &= \max(0, B - 4) \times \max(0, 116.8 - q_{net}) \\
&= \max(14.5 - 4) \times \max(0, 116.8 - 100) \\
&= 176.4, c_m^5 = -0.025 \\
\bullet B_6(x) &= \max(0, 4 - B) \times \max(0, N_c - 18) \\
&= \max(4 - 14.5) \\
&\times \max(0, 6 - 18) = 0, c_m^6 = -2.772 \\
\bullet B_7(x) &= \max(0, 4 - B) \times \max(0, 18 - N_c) \\
&= \max(4 - 14.5) \\
&\times \max(0, 18 - 6) = 0, c_m^7 = -1.652 \\
\bullet B_8(x) &= \max(0, 4 - B) \times \max(0, N_c - 20) \\
&= \max(4 - 14.5) \\
&\times \max(0, 6 - 20) = 0, c_m^8 = -2.734 \\
\bullet B_9(x) &= \max(0, B - 4) \times \max(0, 24 - N_c) \\
&= \max(14.5 - 4) \\
&\times \max(0, 24 - 6) = 189, c_m^9 = 0.151 \\
\bullet B_{10}(x) &= \max(0, B - 4) \times \max(0, 0.13 - D_f/B) \\
&= \max(14.5 - 4) \\
&\times \max(0, 0.13 - 0.07) = 0.63, c_m^{10} \\
&= -8.211
\end{aligned}$$

Therefore, the settlement of given foundation can be predicted as:

$$\begin{aligned}
S_c &= 10.682 + 0.286 \times B_2(x) + 3.642 \times B_3(x) + 0.028 \\
&\times B_4(x) - 0.025 \times B_5(x) + 0.151 \\
&\times B_9(x) + 8.211 \times B_{10}(x)
\end{aligned}$$

$$\begin{aligned}
S_c &= 10.682 + 0.286 \times 10.5 + 3.642 \times 6 + 0.028 \times 600 \\
&- 0.025 \times 176.4 + 0.151 \times 189 \\
&+ 8.211 \times 0.63
\end{aligned}$$

$$S_c = 81.6 \text{ mm}$$

The calculated settlement can be acceptable with an error of only 10.3% compared to the measured settlement of 74 mm, which was reported by Burland and Burbidge (1985).

To demonstrate the predictability of the proposed MARS model, four field tests were selected for verification of Eq. (23) by estimating and comparing settlement of shallow foundation. The two of 3×3 m (Exp No. 1) and 1.82×1.82 (Exp No. 2) m footings were implemented at Riverside Campus of A & M Texas University by Briaud and Gibbens (1994), and Anderson *et al.* (2007), respectively. Two underlain shallow foundations of two buildings (D2 and E1 – Exp No.3 and 4) located in Mascali, Italy were examined by Maugeri *et al.* (1998). Table 8 gives a comparison between the measured settlements from these field tests with the predicted settlements. It is evident that this study's proposed equation provides the best accurate results compared to other methods. The results of this study compared to those of tests performed good predictability for experiment No.1 to 4 with a small error of 5.1, 6.6, 1.6, and 18.5%, respectively.

## 7. Conclusions

This study aimed to propose a novel model with an

explicit formulation for predicting settlement of shallow foundations on sandy soils. This study combined a GA algorithm with MARS to develop a new hybrid model GA-MARS. Further, a new prediction equation was derived for practical calculations. In order to propose the model, a database containing 180 shallow foundation tests with a total of five input variables was collected. Based on the discussion above and comparisons of the proposed model with available methods, some conclusions can be given, as follow:

- It was found that the MARS model can be efficiently utilized to develop an empirical formulation for predicting the settlement of shallow foundations on sandy soils using standard penetration tests. Moreover, the derived formulation can be employed as a handy prediction tool with satisfactory predictability. However, since its expression is rather cumbersome and complex, it is better to transfer this model to a computer to save time and minimize errors.

- Constructing a MARS model with various parameter choices is a complicated and challenging process. The three most important parameters must be considered, including the maximum basis function (max terms)  $M_{max}$ , maximum interaction  $I_{max}$ , and penalty value  $d$ . To obtain the optimal model, a hybrid model should be used for finding the best combination of parameters. This paper illustrated that GA could perform successfully for determining optima value in a high dimensional search space.

- The GA-MARS model is able to provide the relative importance of the input variables based on ANOVA decomposition. Among five-input variables, the two most significant variables were the bread of foundation ( $B$ ) and the blow count of SPT ( $N_c$ ). Conversely, the least important variable was the length to width ( $L/B$ ), which was removed through ANOVA decomposition.

- To assess the relative performance of the GA-MARS model in predicting settlement, this study compared MARS against three traditional methods and another artificial intelligent technique – ANN. Results illustrated that the GA-MARS has superior predictability providing a measured-to-predicted value ratio of close to 1 as well as very low values of  $MAE$  and  $RMSE$ .

- It should be noted that since the developed GA-MARS model predicts based on the knot values and the basis function, thus interpolation between the knots of input variables are more accurate and reliable than extrapolations. Moreover, the range of applicability of the MARS' derived equation is constrained by the data used in the model. Consequently, for cases in which the input variable values are beyond this range, the proposed GA-MARS model should be used with caution. To update the model and make it more robust in the future, it would be desirable to increase the number of data samples so that the model can be re-trained.

## Acknowledgments

This research was supported by Ministry of Land, Infrastructure and Transport of Korean Government (Grant 20CTAP-C143093-03).

## Declaration of conflicting interests

The author(s) declare no potential conflicts of interest concerning the research, authorship, and/or publication of this article.

## References

- Abate, G., Caruso, C., Massimino, M.R. and Maugeri, M. (2008), "Evaluation of shallow foundation settlements by an elastoplastic kinematic-isotropic hardening numerical model for granular soil", *Geomech. Geoenviron. Eng.*, **3**(1), 27-40. <https://doi.org/10.1080/17486020701862174>.
- Alpan, I. (1964), "Introductory Soil mechanics and foundations / G.B. Sowers, G.F. Sowers", *Civ. Eng. Public Work. Rev.*, **58**, 1415-1418. <https://doi.org/10.1097/00010694-195111000-0014>.
- Anagnostopoulos, A.G., Papadopoulos, B.P. and Kavvadas, M.J. (1991), "Direct estimation of settlements on sand, based on SPT results", *Proceedings of the 10th European Conference on Soil Mechanics and Foundation Engineering*, Florence, Italy.
- Anderson, J.B., Townsend, F.C. and Rahelison, L. (2007), "Load testing and settlement prediction of shallow foundation", *J. Geotech. Geoenviron. Eng.*, **133**(12), 1494-1502. [https://doi.org/10.1061/\(ASCE\)1090-0241\(2007\)133:12\(1494\)](https://doi.org/10.1061/(ASCE)1090-0241(2007)133:12(1494)).
- Arnold, M. (1980), "Prediction of footing settlement on sand", *Ground Eng.*, **13**, 40-47.
- Briaud, J.L. and Gibbens, R.M. (1994), "Predicted and measured behavior of five spread footings on sand", *Geotech. Sp. Publ.*, **41**, 255.
- Bui, D.K., Nguyen, T., Chou, J.S., Nguyen-Xuan, H. and Ngo, T. D. (2018), "A modified firefly algorithm-artificial neural network expert system for predicting compressive and tensile strength of high-performance concrete", *Constr. Build. Mater.*, **180**, 320-333. <https://doi.org/10.1016/j.conbuildmat.2018.05.201>.
- Bui, D.K., Nguyen, T.N., Ngo, T.D. and Nguyen-Xuan, H. (2019), "An artificial neural network (ANN) expert system enhanced with the electromagnetism-based firefly algorithm (EFA) for predicting the energy consumption in buildings", *Energy*, **190**, 116370. <https://doi.org/10.1016/j.energy.2019.116370>.
- Burland, J.B. and Burbidge, M.C. (1985), "Settlement of foundations on sand and gravel", *Proc. Inst. Civ. Eng.*, **78**(6), 1325-1381.
- Cheng, M.Y. and Cao M.T. (2014), "Evolutionary multivariate adaptive regression splines for estimating shear strength in reinforced-concrete deep beams", *Eng. Appl. Artif. Intell.*, **28**, 86-96. <https://doi.org/10.1016/j.engappai.2013.11.001>.
- Craven, P. and Wahba, G. (1978), "Smoothing noisy data with spline functions", *Numer. Math.*, **31**(4), 377-403. <https://doi.org/10.1007/BF01404567>.
- Das, B. and Sivakugan, N. (2007), "Settlements of shallow foundations on granular soil — an overview", *Int. J. Geotech. Eng.*, **1**(1), 19-29. <https://doi.org/10.3328/IJGE.2007.01.01.19-29>.
- Das, B.M. (2002), *Principles of Foundation Engineering*, Cengage Learning, U.S.A.
- Elton, D.J. (1987), "Settlement of footings on sand by CPT data", *J. Comput. Civ. Eng.*, **1**(2), 99-113. [https://doi.org/10.1061/\(ASCE\)0887-3801\(1987\)1:2\(99\)](https://doi.org/10.1061/(ASCE)0887-3801(1987)1:2(99)).
- Friedman, J.H. (1991), "Multivariate adaptive regression splines", *Ann. Statist.*, **19**(1), 1-67.
- Gandomi, A.H., Alavi, A.H. and Sahab, M.G. (2010), "New formulation for compressive strength of CFRP confined concrete cylinders using linear genetic programming", *Mater. Struct.*, **43**(7), 963-983. <https://doi.org/10.1617/s11527-009-9559-y>.
- Gesoglu, M. and Güneyisi, E. (2007), "Prediction of load-carrying capacity of adhesive anchors by soft computing techniques", *Mater. Struct.*, **40**(9), 939-951. <https://doi.org/10.1617/s11527-007-9265-6>.
- Golafshani, E.M., Rahai, A. and Sebt, M.H. (2015), "Artificial neural network and genetic programming for predicting the bond strength of GFRP bars in concrete", *Mater. Struct.*, **48**(5), 1581-1602. <https://doi.org/10.1617/s11527-014-0256-0>.
- Goldberg, D.E. (1989), *Genetic Algorithms in Search, Optimization and Machine Learning*, 1st Ed., Addison-Wesley Longman Publishing Co., Inc., Boston, Massachusetts, U.S.A.
- Gomes, G.F., de Almeida, F.A., Junqueira, D.M., da Cunha Jr, S. S. and Ancelotti Jr, A.C. (2019), "Optimized damage identification in CFRP plates by reduced mode shapes and GA-ANN methods", *Eng. Struct.*, **181**, 111-123. <https://doi.org/10.1016/j.engstruct.2018.11.081>.
- Harr, M.E. (1966), *Foundation and Theoretical Soil Mechanics*, McGraw-Hill, New York, U.S.A.
- Holland, J.H. (1975), *Adaptation in Natural and Artificial Systems: An Introductory Analysis with Applications to Biology, Control, and Artificial Intelligence*, U Michigan Press, Oxford, England, U.K.
- Iyer, V.H., Mahesh, S., Malpani, R., Sapre, M. and Kulkarni, A.J. (2019), "Adaptive range genetic algorithm: A hybrid optimization approach and its application in the design and economic optimization of shell-and-tube heat exchanger", *Eng. Appl. Artif. Intell.*, **85**, 444-461. <https://doi.org/10.1016/j.engappai.2019.07.001>.
- Jeyepalan, J.K. and Boehm, R. (1986), *Procedures for Predicting Settlement in Sands*, in *Settlement of Shallow Foundations on Cohesionless Soils: Design and Performance*, American Society of Civil Engineers, 1-22.
- Koopialipour, M., Fallah, A., Armaghani, D.J., Azizi, A. and Mohamad, E.T. (2019), "Three hybrid intelligent models in estimating flyrock distance resulting from blasting", *Eng. Comput.*, **35**(1), 243-256. <https://doi.org/10.1007/s00366-018-0596-4>.
- Le-Duc, T., Nguyen, Q.H. and Nguyen-Xuan, H. (2020), "Balancing composite motion optimization", *Inform. Sci.*, **520**, 250-270. <https://doi.org/10.1016/j.ins.2020.02.013>.
- Luat, N.V., Lee, J., Lee, D.H. and Lee, K. (2020b), "GS - MARS method for predicting the ultimate load - carrying capacity of rectangular CFST columns under eccentric loading", *Comput. Concrete*, **25**(1), 1-14. <https://doi.org/10.12989/cac.2020.25.1.001>.
- Luat, N.V., Lee, K. and Thai, D.K. (2020a), "Application of artificial neural networks in settlement prediction of shallow foundations on sandy soils", *Geomech. Eng.*, **20**(5), 385-397. <https://doi.org/10.12989/gae.2020.20.5.385>.
- Maugeri, M., Castelli, F., Massimino, M.R. and Verona, G. (1998), "Observed and computed settlements of two shallow foundations on sand", *J. Geotech. Geoenviron. Eng.*, **124**(7), 595-605. [https://doi.org/10.1061/\(ASCE\)1090-0241\(1998\)124:7\(595\)](https://doi.org/10.1061/(ASCE)1090-0241(1998)124:7(595)).
- Meyerhof, G. (1956), "Penetration tests and bearing capacity of cohesionless soils", *J. Soil Mech. Found. Div.*, **82**(1), 1-12.
- Meyerhof, G. (1964), "Shallow foundations", *J. Soil Mech. Found. Div.*, **91**, 21-32.
- Meyerhof, G. (1974), "General report: State-of-the-art of penetration testing in countries outside Europe", *Proceedings of the 1st European Symposium on Penetration Testing*, Stockholm, Sweden.
- Mullins, G., Winters, D. and Dapp, S. (2006), "Predicting end bearing capacity of post-grouted drilled shaft in cohesionless soils", *J. Geotech. Geoenviron. Eng.*, **132**(4), 478-487. [https://doi.org/10.1061/\(ASCE\)1090-0241\(2006\)132:4\(478\)](https://doi.org/10.1061/(ASCE)1090-0241(2006)132:4(478)).

- Nehdi, M. and Nikopour, H. (2011), "Genetic algorithm model for shear capacity of RC beams reinforced with externally bonded FRP", *Mater. Struct.*, **44**(7), 1249-1258. <https://doi.org/10.1617/s11527-010-9697-2>.
- Pramanik, P. and Maiti, M.K. (2019), "An inventory model for deteriorating items with inflation induced variable demand under two level partial trade credit: A hybrid ABC-GA approach", *Eng. Appl. Artif. Intell.*, **85**, 194-207. <https://doi.org/10.1016/j.engappai.2019.06.013>.
- Qi, C. and Tang, X. (2018), "A hybrid ensemble method for improved prediction of slope stability", *Int. J. Numer. Anal. Meth. Geomech.*, **42**(15), 1823-1839. <https://doi.org/10.1002/nag.2834>.
- Ren, Y. and Bai, G. (2010), "Determination of optimal SVM parameters by using GA/PSO", *J. Comput.*, **5**(8), 1160-1168. <https://doi.org/10.4304/jcp.5.8.1160-1168>.
- Samui, P. (2011), "Multivariate adaptive regression spline applied to friction capacity of driven piles in clay", *Geomech. Eng.*, **3**(4), 285-290. <https://doi.org/10.12989/gae.2011.3.4.285>.
- Samui, P. and Sitharam, T.G. (2008), "Least-square support vector machine applied to settlement of shallow foundations on cohesionless soils", *Int. J. Numer. Anal. Meth. Geomech.*, **32**(17), 2033-2043. <https://doi.org/10.1002/nag.731>.
- Schmertmann, J.H. (1970), "Static cone to compute static settlement over sand", *J. Soil Mech. Found. Div.*, **96**(3), 1011-1043.
- Schultze, E. and Sherif, G. (1973), "Prediction of settlements from evaluated settlement observations for sand", *Proceeding of the 8th International Conference on Soil Mechanics and Foundation Engineering*, Moscow, Russia, August.
- Shahin, M., Jaksa, M.B. and Maier, H.R. (2005), "Neural network based stochastic design charts for settlement prediction", *Can. Geotech. J.*, **120**, 110-120. <https://doi.org/10.1139/T04-096>.
- Shahin, M.A. and Jaksa, M.B. (2006), "Pullout capacity of small ground anchors by direct cone penetration test methods and neural networks", *Can. Geotech. J.*, **43**(6), 626-637. <https://doi.org/10.1139/t06-029>.
- Shahin, M.A., Maier, H.R. and Jaksa, M.B., (2002), "Predicting settlement of shallow foundations using neural networks", *J. Geotech. Geoenviron. Eng.*, **128**(9), 785-793. [https://doi.org/10.1061/\(ASCE\)1090-0241\(2002\)128:9\(785\)](https://doi.org/10.1061/(ASCE)1090-0241(2002)128:9(785)).
- Sivakugan, N. and Johnson, K. (2004), "Settlement predictions in granular soils: a probabilistic approach", *Géotechnique*, **54**(7), 499-502. <https://doi.org/10.1680/geot.2004.54.7.499>.
- Tan, C.K. and Duncan, J.M. (1991), "Settlement of footings on sands: Accuracy and reliability", *Proceedings of the Geotechnical Engineering Congress*, Boulder, Colorado, U.S.A., June.
- Terzaghi, K. and Peck, R.B. (1968), *Soil Mechanics in Engineering Practice*, John Wiley & Sons, New York, U.S.A.
- Tiachacht, S., Bouazzouni, A., Khatir, S., Abdel Wahab, M., Behtani, A. and Capozucca, R. (2018), "Damage assessment in structures using combination of a modified Cornwell indicator and genetic algorithm", *Eng. Struct.*, **177**, 421-430. <https://doi.org/10.1016/j.engstruct.2018.09.070>.
- Wang, Y., Huang, H., Huang, L. and Zhang, X. (2018), "Source term estimation of hazardous material releases using hybrid genetic algorithm with composite cost functions", *Eng. Appl. Artif. Intell.*, **75**, 102-113. <https://doi.org/10.1016/j.engappai.2018.08.005>.
- Xiang, Y., Goh, A.T.C., Zhang, W. and Zhang, R. (2018), "A multivariate adaptive regression splines model for estimation of maximum wall deflections induced by braced excavation", *Geomech. Eng.*, **14**(4), 315-324. <https://doi.org/https://doi.org/10.12989/gae.2018.14.4.315>.
- Zhang, W. and Goh, A.T.C. (2014), "Multivariate adaptive regression splines model for reliability assessment of serviceability limit state of twin caverns", *Geomech. Eng.*, **7**(4), 431-458. <https://doi.org/10.12989/gae.2014.7.4.431>.
- Zhang, W., Zhang, R. and Goh, A.T.C. (2018), "MARS inverse analysis of soil and wall properties for braced excavations in clays", *Geomech. Eng.*, **16**(6), 577-588. <https://doi.org/10.12989/gae.2018.16.6.577>.
- Zhang, W., Zhang, R., Wang, W., Zhang, F. and Goh, A.T.C. (2019), "A multivariate adaptive regression splines model for determining horizontal wall deflection envelope for braced excavations in clays", *Tunn. Undergr. Sp. Technol.*, **84**, 461-471. <https://doi.org/10.1016/j.tust.2018.11.046>.

GC